




Analyzing spatial variance of urban waterlogging disaster at multiple scales based on a hydrological and hydrodynamic model

Luoyang Wang^{1,2} · Yao Li⁴ · Hao Hou^{1,2,3} · Yan Chen^{1,2} · Jinjin Fan^{1,2} · Pin Wang^{1,2,3} · Tangao Hu^{2,3} 

Received: 23 January 2022 / Accepted: 15 June 2022 / Published online: 5 July 2022
© The Author(s), under exclusive licence to Springer Nature B.V. 2022

Abstract

The frequency of urban waterlogging is increasing significantly under the combined influence of natural factors (precipitation and terrain) and anthropogenic factors (drainage system and urbanization). Previous studies had explored the effect of landscape pattern and topography on waterlogging based on historical waterlogging events records. However, the research on current waterlogging issues based on historical records had limitations since the impact factors of waterlogging are inconsistent due to the changes of surface and meteorological conditions. This paper applied a hydrological and hydrodynamic model named InfoWorks ICM, to simulate the urban waterlogging depth (UWD). Under the consistent surface and meteorological conditions, UWD were selected as the dependent variable to analyze the influence of landscape pattern and topography on waterlogging at multiple scales. Pearson correlation analysis and stepwise regression models were used to discover the relationship between these indices. According to the results, in terms of landscape composition, the percentages of built-up area and urban green space have the most significant influence on waterlogging. In addition, organizing average built-up area patch sizes and integrating green spaces with complex shape and high connectivity can improve the state of urban waterlogging. Besides, the rational allocation of topographic gradient is an effective measure at small scale. The adjusted R^2 of regression model were 0.723 at 400 m analysis scale, 0.323 at 600 m analysis scale, and 0.193 at 800 m analysis scale, indicating that attention should be paid to scale effect in similar research. This research can provide a reference for mitigating urban waterlogging disasters.

Keywords Urban waterlogging · InfoWorks ICM · Landscape composition and configuration · Terrain · Disaster reduction

✉ Tangao Hu
hutangao@hznu.edu.cn

Extended author information available on the last page of the article

1 Introduction

Urban waterlogging refers to the disaster of stagnant water disaster in the urban area due to a heavy or continuous precipitation exceeding the urban drainage capacity (Xue et al. 2016; Yu et al. 2018). In the context of global climate change, the frequency of extremely heavy and long-term rainfall increased significantly around the world, causing an increase in the probability of waterlogging events (Kirtman et al. 2013). Furthermore, in the process of urbanization, the impervious surface expands rapidly, which changes the process of water cycle on the original surface and further aggravates the waterlogging risk, especially in low-lying coastal cities (Sang and Yang 2017; Liu et al. 2019).

China, as one of the largest developing countries, experienced a massive city expansion since the government introduced the open-door policy in 1978. Simultaneously, China is suffering extensively from the environmental impacts of rapid urbanization and climate change (Huang et al. 2017; Hou et al. 2019). According to the “*Statistical Bulletin of Flood and Drought Disasters in China*” from the Ministry of Water Resources of the People’s Republic of China, an average of 2065 cities experienced urban waterlogging from 2006 to 2020, especially the economically developed cities in east of China, which have big population and developed economy (<http://www.mwr.gov.cn/>). Previous studies have shown that the urban waterlogging will cause huge economic losses and casualties, threaten traffic safety, paralyze the basic functions of cities, affect water quality and damage the ecological environment et.al (Su et al. 2016; Tang et al. 2018; Fahy et al. 2019). For example, according to the disaster investigation report by the Ministry of Emergency Management of the People’s Republic of China (<https://www.mem.gov.cn/>), on July 20, 2021, Zhengzhou city suffered the heaviest rainfall on record (449 mm), causing traffic paralysis and communication interruption, and resulting in 380 casualties and economic losses of 40.9 billion yuan. Therefore, how to solve the urban waterlogging has become a heated topic discussed by scholars and the public in the process of sustainable urban development in China.

Considerable researches have shown that most waterlogging events are caused by both natural factors and human activities (Zhang et al. 2017; Wang et al. 2021). In terms of natural factors, in addition to the extreme precipitation caused by global climate change, the “urban rain island” effect which means the precipitation in urban is higher than suburbs is also a major factor (Zhao et al. 2021). Besides, urban micro-topography is also an important natural factor causing waterlogging events, due to its effect on runoff (Huong and Pathirana 2013; Wu et al. 2020). Among anthropogenic factors, low designed standards and inadequate management of drainage facilities lead the loss of urban drainage function during heavy rainstorms, and result in waterlogging (Zhang et al. 2021c). And the changes in landscape pattern (composition and configuration) especially the expansion of impervious surface and the reducing of green space caused by urbanization also effectively promote the frequent occurrence of waterlogging (Yao et al. 2017; Zhang et al. 2018b). Among these factors, the researches on analyzing impact factors of waterlogging from the landscape pattern and urban micro-topography are mostly did.(Wu and Zhang 2017; Yu et al. 2018; Zhang et al. 2018a, 2020; Zhao et al. 2018; Tehrany et al. 2019; Liu et al. 2021), and these studies used the historical waterlogging records to characterize urban waterlogging. Historical waterlogging points are true reflection of past waterlogging events. In order to ensure that there are enough samples for statistical analysis, records of many years are usually needed. Under the rapid change of urban surface conditions, it is inaccurate to use historical waterlogging points and the latest surface conditions to analyze the impact factors. More importantly, the scale of these studies based on historical

waterlogging points is usually at the level of large watersheds. In this context, the relationship between waterlogging events and their impact factors can be well obtained, but the related results and findings will be hard to implement in terms of feasibility due to the large spatial level.

At present, the hydrological and hydrodynamic models are extensively utilized to simulate the urban waterlogging process, such as Storm Water Management Model (SWMM), MIKE Urban, and InfoWorks Integrated Catchment Model (ICM) (Bisht et al. 2016; Nayeb Yazdi et al. 2019). These models could solve the problem mentioned above; however, the research applied the hydrological and hydrodynamic models to analyze the influence of topography and landscape pattern on urban waterlogging is lacking. As one of the representative one-dimensional (1D) hydrological models, the SWMM was widely used to analyze the process caused by runoff (Burger et al. 2014; Babaei et al. 2018); however, it cannot reflect the surface water flows directly (Zhang et al. 2021b). On the other hand, the InfoWorks ICM combined the one-dimensional (1D) hydraulic model of urban drainage networks and the two-dimensional (2D) flood inundation model of the urban catchment. Thus, it could simulate the situation of water flows on the surface and with higher accuracy than SWMM (Zhang et al. 2021a). Comparing to the other one-dimensional and two-dimensional coupled model, such as MIKE Urban, InfoWorks ICM has an embedded Structure Query Language (SQL) system that can make data pre- and post-processing more convenient (Song et al. 2021). More importantly, since InfoWorks ICM could invoke GPU to participate in simulation, it has higher efficiency, especially in the simulation of drainage network model with large amount of data (H. Wallingford 2012). Therefore, InfoWorks ICM is widely used for urban waterlogging disaster and risk mapping studies (Cheng et al. 2017; Sidek et al. 2021). Considering the significant advantages of InfoWorks ICM, this study utilized this model to simulate the process of urban waterlogging and took the result of urban waterlogging depth (UWD) as the dependent variable. Meanwhile, considering the complexity of urban waterlogging, this study took landscape indices and topographic indices as the independent variables in the regression model, to obtain a more comprehensive result on the relationship.

The main objective of this study is to provide useful information to reduce the effect of urban waterlogging. In order to accomplish the main objective, our targets included: (1) simulate the UWD in the process of a rainfall and obtain its spatial distribution; (2) detect the relationships between the urban waterlogging and landscape pattern and topography at multiple scales; (3) summarize the causes and solutions of the urban waterlogging problems in the study area from the perspective of landscape and topographic planning.

2 Materials and methods

2.1 Study area

Haining City is located in the plain near Hangzhou Bay, north bank of Qiantang River, Zhejiang Province, P.R China, at 30°15′–30°35′ N and 120°18′–120°52′ E (Fig. 1). The municipal area of Haining City is 863.32 km², and the urban area is 150.52 km² (<http://www.haining.gov.cn/>). The annual average precipitation in Haining reaches 1187 mm, with the influence of subtropical monsoon climate and typhoon. The rainy season of Haining is mainly in summer (Li et al. 2019). More specifically, June–July is Meiyu season and July–September is typhoon season, in which characteristics of rainfall are long duration

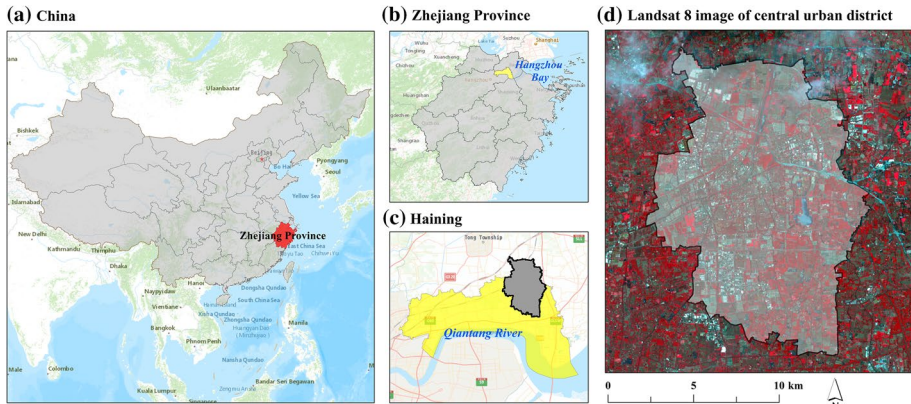


Fig. 1 The location of Haining central urban district

and high intensity. Meanwhile, the topography of Haining is flat, the percentage of plain is greater than 80%, and the mean elevation of study area is less than 20 m. Thus, waterlogging occurs frequently in this region during rainy season, especially in central urban district with more impervious surface and less green space than rural area.

According to the record of China Meteorological Administration, the residents in Haining suffered a serious waterlogging disaster caused by heavy rainfall (94.2 mm/h) on September 16, 2018 (<http://www.cma.gov.cn/>). And in the first national survey of natural disasters in China, waterlogging was listed as one of the most serious problems in Haining. Therefore, this study selected central urban district of Haining which with high frequency of urban waterlogging as study area. More importantly, the study in Haining could provide reference for other plain cities located in southeastern China.

2.2 Data collection and pre-processing

In this study, we utilized Haining administrative division data, 1:5000 unmanned aerial vehicle (UAV) image and land use survey data to determine the land cover in 2016. For the edge of study area which is lack of UAV image, the Landsat 8 OLI/TIRS images were used to determine the land cover information. The ASTER GDEM, urban drainage network, precipitation records and measured flow data were used to simulate urban waterlogging and evaluate the simulation results. The detailed information of the dataset is shown in Table 1.

The main work of data pre-processing was urban drainage network simplification which had a significant effect on simulation efficiency. According to the idea of linking the area of property with the pipe mentioned in pervious study (Abbas et al. 2019), we simplified the data of urban drainage network without affecting the original effect of the network. The number of urban drainage nodes and lines was 2916 and 2417 after simplification.

2.3 Overall workflow

This study attempted to detect the impact factors of urban waterlogging from the perspectives of landscape pattern and terrain. The overall workflow was designed as follows

Table 1 Description of the data used in study

Data name	Year	Source
<i>Vector data</i>		
Haining administrative divisions	2021	Haining natural resources bureau
Land use survey data	2016	Haining natural resources bureau
Urban drainage network	2016	Haining city administration bureau
<i>Text data</i>		
Meteorological precipitation records	2018	Haining city administration bureau
Flowmeter measurement records	2018	Field survey
<i>Raster data</i>		
1:5000 UAV image	2016	Haining natural resources bureau
Landsat 8 OLI/TIRS image	2016	United states geological survey (USGS)
ASTER GDEM	2013	National aeronautics and space administration (NASA)

The acquisition date of UAV image is 26 June, 2016. The acquisition date and time of Landsat 8 OLI/TIRS image is 23 June, 2016 (10:31:27), the path is 119, and the raw is 39

(Fig. 2), with five main part works: (1) urban waterlogging stimulation based on urban drainage network, precipitation and DEM in InfoWorks ICM, (2) terrain factors calculation based on ASTER GDEM in ArcGIS 10.4, (3) land cover mapping based on UAV image,

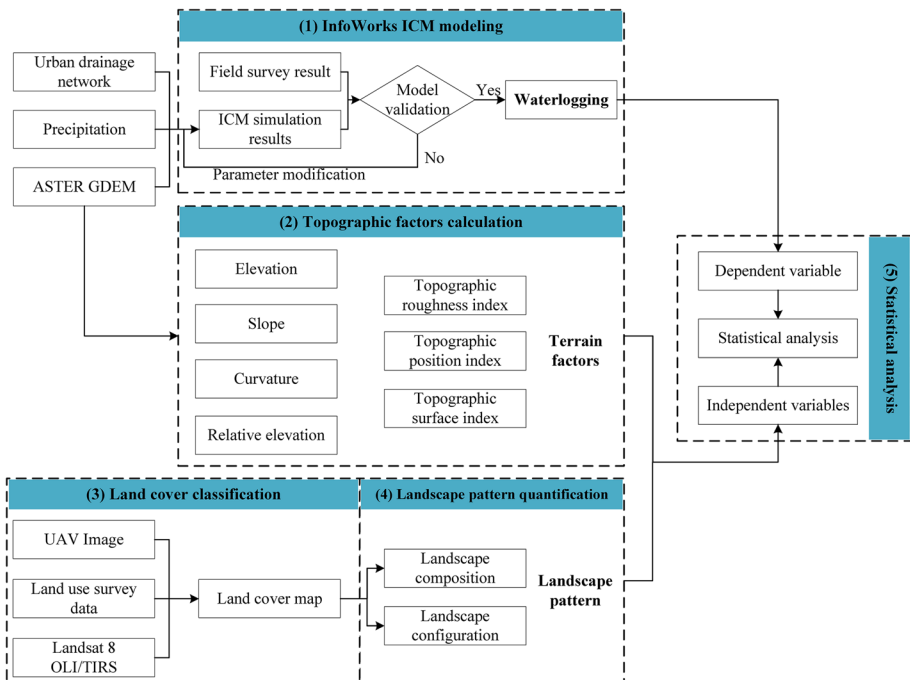


Fig. 2 The overall workflow of study

land use survey data and Landsat 8 OLI/TIRS in ArcGIS10.4 and ENVI 5.3, (4) quantification the landscape pattern (composition and configuration) based on land cover map obtained in part 3 in FRAGSTATS 4.2, (5) statistical analysis of urban waterlogging based on landscape pattern and terrain factors.

2.4 Urban waterlogging simulation

2.4.1 InfoWorks ICM

InfoWorks ICM, a coupled hydrological and hydrodynamic model developed by Innovyze®, was adapted to simulate urban waterlogging. The flexible data exchange capability of InfoWorks ICM and parallel computation based on GPUs improved the simplicity and computational efficiency in two-dimensional hydrodynamic modeling greatly (Yang et al. 2021). The runoff calculation and flow convergence for the hydrological model, one-dimensional hydrodynamic simulation for the underground pipe networks, and the two-dimensional hydrodynamic simulation for surface inundation are included in whole process of waterlogging simulation. The hydrodynamic simulation for the underground pipe networks is implemented by solving the Saint–Venant equations. The Preissmann Slot is used to calculate complicated hydraulic conditions including surface flow and pressurized flow two states (Cheng et al. 2017). The Saint–Venant formulas are as follows:

$$\frac{\partial A}{\partial t} + \frac{\partial Q}{\partial x} = 0 \quad (1)$$

$$\frac{\partial Q}{\partial t} + \frac{\partial}{\partial x} \left(\frac{Q^2}{A} \right) + gA \left(\cos \theta \frac{\partial h}{\partial x} - S_0 + \frac{Q|Q|}{K^2} \right) = 0 \quad (2)$$

where A is the cross-sectional area of the pipe (m^2), Q is the flow rate of the pipe (m^3/s), t is time (s), x is the length along the x direction (m), h is water depth (m), g is the gravitational acceleration (m^2/s), θ is the angle between the pipe line and horizontal line (degree), and S_0 and K are the bed slope and conveyance, respectively.

The mathematical representation of the 2D surface flow is based on the nonlinear shallow water equations. It is a simplified form obtained by averaging the Navier–Stokes equation in the direction of water depth (YE et al. 2021). It was used for two-dimensional hydrodynamic simulation. The formulas are as follows:

$$\frac{\partial h}{\partial t} + \frac{\partial(hu)}{\partial x} + \frac{\partial(hv)}{\partial x} = q_{1D} \quad (3)$$

$$\frac{\partial(hu)}{\partial t} + \frac{\partial}{\partial x} \left(hu^2 + \frac{gh^2}{2} \right) + \frac{\partial(huv)}{\partial y} = -gh(S_{0,x} - S_{f,x}) + q_{1D}u_{1D} \quad (4)$$

$$\frac{\partial(hv)}{\partial t} + \frac{\partial}{\partial x} \left(hv^2 + \frac{gh^2}{2} \right) + \frac{\partial(huv)}{\partial y} = -gh(S_{0,y} - S_{f,y}) + q_{1D}v_{1D} \quad (5)$$

where u and v are velocities in x and y directions (m/s), respectively, q_i is the source discharge per unit area (m/s), u_i and v_i are the velocity components of the source discharge in x

and y directions (m/s), respectively, $S_{0,x}$ and $S_{0,y}$ are the ground slope in x and y directions, respectively, and $S_{f,x}$ and $S_{f,y}$ are the friction slopes in x and y directions, respectively.

2.4.2 Model construction

The study area was generalized as urban plain catchment area in the model according to its characteristic of underlying surface. In this study, the whole study area was divided into eight primary catchments according to the distribution of river, road and urban drainage network. After that, each primary catchment was divided into sub-catchments based on Thiessen polygon which was created by urban drainage node. Besides, the land cover type in each sub-catchment includes built-up area, road and avenue, urban green space, farmland and water. The attributes of each land cover are listed in Table 2. These parameters are set and adjusted mainly referring to the InfoWorks ICM help document (H. Wallingford 2012), Storm Water Management Model (SWMM) help document (Rossman 2015) and designed standard for outdoor drainage by Ministry of Housing and Urban–Rural Development of China in 2014.

2.4.3 Model calibration and validation

In this study, the flowmeter measurement records during the rainfall on 20 August, 2018, were used to verify the reliability of the model. By comparing the measured data obtained by flowmeter and simulation data obtained by the model of two observed stations in the study area (Fig. 3a, b), the RMSE was $0.005 \text{ m}^3/\text{s}$ and $0.003 \text{ m}^3/\text{s}$, respectively, indicating that the model could simulate waterlogging accurately and effectively.

2.5 Explanatory variables

Previous researches showed that the landscape pattern, topographic factors and urban drainage network have a significant impact on urban waterlogging events (Wu and Zhang 2017; Tehrany et al. 2019; Zhang et al. 2020). Owing to the use of urban drainage network data in the waterlogging simulation, it was not taken as an explanatory variable in order to prevent the possible impact of this modus operandi on the results. Thus, totally 18 explanatory variables were considered in this study.

2.5.1 Landscape composition

Landscape composition refers to the percentage of each land cover types (PLAND) within the landscape (Du et al. 2016). In this study, the land cover data were classified from land use survey data, UAV image and Landsat 8 OLI/TIRS image, and they were divided into five categories: (1) built-up area (including house, buildings and squares); (2) road and avenue (RAV); (3) water (including lake, pond and river); (4) urban green space (UGS, including grassland and forest); and (5) farmland (including vegetable field and paddy field).

2.5.2 Landscape configuration

Landscape configuration refers to the spatial characteristics, arrangement, position or geometric complexity of landscape (Wang et al. 2020). It has been proven that landscape metrics, such as the index of shape, complexity and aggregation, are able to

Table 2 Parameter attributes for five land cover types

Land cover	Surface type	Runoff model	Runoff coef- ficient	Initial losses type	Initial losses (m)	Routine model	Routine parameter
Built-up area	Impervious surface	Fixed	0.95	Constant	0.001	SWMM	0.02
Road and avenue	Impervious surface	Fixed	0.9	Constant	0.002	SWMM	0.02
Urban green space	Pervious surface	Fixed	0.2	Constant	0.0025	SWMM	0.05
Farmland	Pervious surface	Fixed	0.15	Constant	0.0025	SWMM	0.045
Water	Impervious surface	Fixed	1	Constant	0	SWMM	0.03

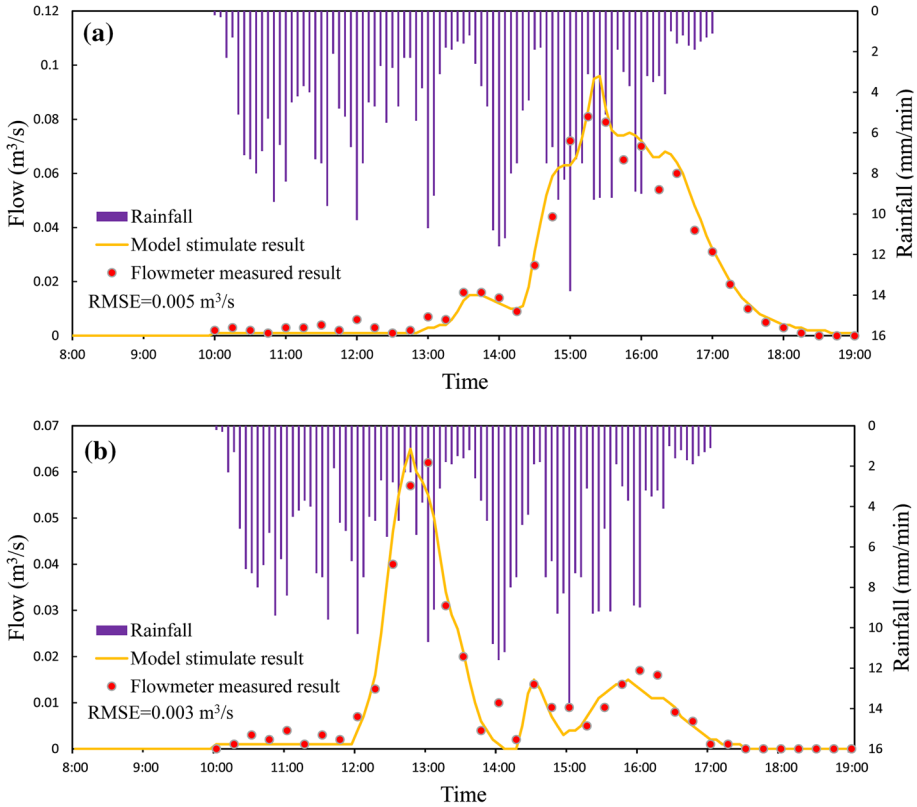


Fig. 3 The simulated result and measured result at **a** observation station 1, **b** observation station 2

explain the spatial heterogeneity of waterlogging events (Huong and Pathirana 2013; Wu et al. 2020). In this study, considering the abilities in reflecting the characteristics of landscape patterns and their simplicity in interpretation, six class-level spatial metrics were selected: largest patch index (LPI), total edge (TE), mean patch area (AREA_MN), mean shape index (SHAPE_MN), patch density (PD), and patch cohesion index (COHESION). The equations and descriptions of these indices are listed in Table 3

2.5.3 Topographic factors

In natural conditions, runoff flows to lower elevations area under the influence of gravity and forms waterlogging. The research around the world has shown the effect of topography to waterlogging events (Wang et al. 2015; Zambrano et al. 2018; Shi et al. 2019). In this study, seven topographic factors, including elevation (Fig. 4a), slope (Fig. 4b), curvature (Fig. 4c), relative elevation (RE), topographic roughness index (TRI, Fig. 4d), topographic position index (TPI, Fig. 4e), and topographic surface texture index (TSI, Fig. 4f), were selected to reflect topographic characters. The equations and descriptions of these factors are listed in Table 3

Table 3 Summary and description of explanatory variables used in study (McGarigal and Marks 1995; Iwahashi and Pike 2007; De Reu et al. 2013; Hu et al. 2021)

Variable	Formula	Description (Unit)
<i>Landscape composition</i>		
PLAND	$PLAND = P_i = \frac{\sum_{j=1}^n a_j}{A}$	Percentage of land cover i within an analysis unit (%)
<i>Landscape configuration</i>		
LPI	$LPI = \frac{\max(a_i)}{A} (100)$	Percentage of the landscape that the largest patch comprises (%)
TE	$TE = \sum_{j=1}^n e_j$	Sum of the lengths of all edge segments involving the corresponding patch type (m)
AREA_MIN	$AREA_MIN = \frac{\sum_{i=1}^n a_i}{10000 \times n}$	Average area of the corresponding patches within an analysis unit (km ²)
SHAPE_MIN	$SHAPE_MIN = \frac{0.25 P_i}{n \sqrt{a_i}}$	Average shape index of the corresponding patches within an analysis unit. Unit (none)
PD	$PD = \frac{(10000)(100)P_i}{A}$	Number of patches of the patch type i per 100 hectares. Unit (none)
COHESION	$COHESION = (100) \times \left[1 - \frac{\sum_{j=1}^n P_{ij}}{\sum_{j=1}^n P_i \sqrt{a_{ij}}} \right] \times \left[1 - \frac{1}{\sqrt{Z}} \right]^{-1}$	Physical connectedness of the corresponding patch type. Unit (none)
<i>Topographic factors</i>		
Elevation	-	Mean elevation within an analysis unit (m)
Slope	-	Mean slope within an analysis unit (degree)
Curvature	-	Mean curvature within an analysis unit (m ⁻¹)
RE	$RE = E_{max} - E_{min}$	Degree of elevation variation within an analysis unit (m)
TRI	$TRI = Y \sqrt{\frac{\sum (x_{ij} - x_{00})^2}{n}}$	Sum change in elevation between a grid cell and its eight neighbor cells. Unit (none)
TPI	$TPI = E_c - E_m$	Difference of elevation between central point and its surrounding region. Unit (m)
TSI	$TSI = \frac{f_{ij}}{\sum N_{ij}}$	Frequency of pits and peaks within adjacent region. Unit (none)

P_i is proportion of the landscape occupied by patch type (class) i, a_i is area (m²) of patch i, n is number of patches, e_j is length (m) of edge involving patch type (class) i, n_i is number of patches of patch type (class) i, P_{ij} is perimeter of patch ij in terms of number of cell surfaces, a_{ij} is area of patch ij in terms of number of cells, Z is total number of cells in the landscape, E_{max} is maximum of elevation, E_{min} is minimum of elevation, $x_{ij} - x_{00}$ is elevation of each neighbor cell to cell (0,0), E_c is elevation of central point, E_m is mean elevation around central point within a predetermined radius, f_{ij} is number of pits or peaks, N_{ij} is total number of pixels

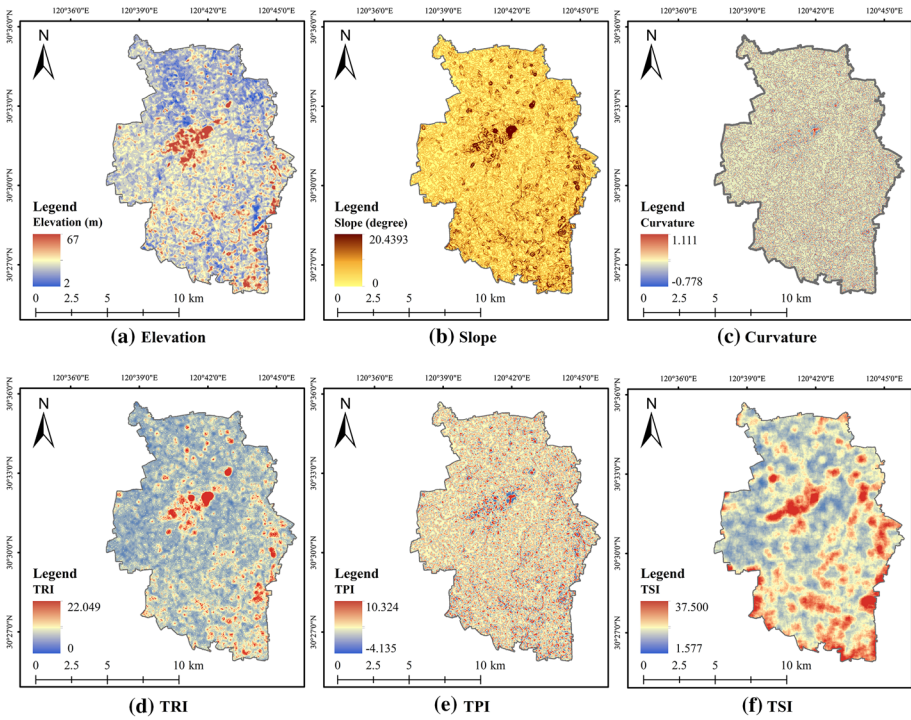


Fig. 4 The a elevation, b slope, c curvature, d TRI, e TP, and f TSI in the study area

2.6 Multiple scales statistical analysis

In this study, Pearson correlation analysis and stepwise regression model were used to detect the impact factors of urban waterlogging. Four scales, 200, 400, 600, and 800 m, were taken as the basic analysis units for statistical analysis. The dependent variable was mean UWD in each grid, while the land cover characteristics (landscape composition and configuration) and topographic factors were included as the explanatory variables. The result of single sample Kolmogorov–Smirnov (KS) indicated that the dataset of each variable was non-normal distribution; thus, these variables were converted into $\ln(X_i)$ before stepwise regression.

The stepwise regression model could eliminate collinearity between variables and has a good performance in multiple regression (Chen et al. 2015; Zheng et al. 2021). The formula of stepwise regression model is as follows:

$$Y = \beta_0 + \beta_1 X_1 + \beta_2 X_2 + \dots + \beta_n X_n \tag{6}$$

where Y is the dependent variable, X_i ($i=1, 2, \dots, n$) is the independent variable, β_0 is the constant, and β_i ($i=1, 2, \dots, n$) is the standard regression coefficient.

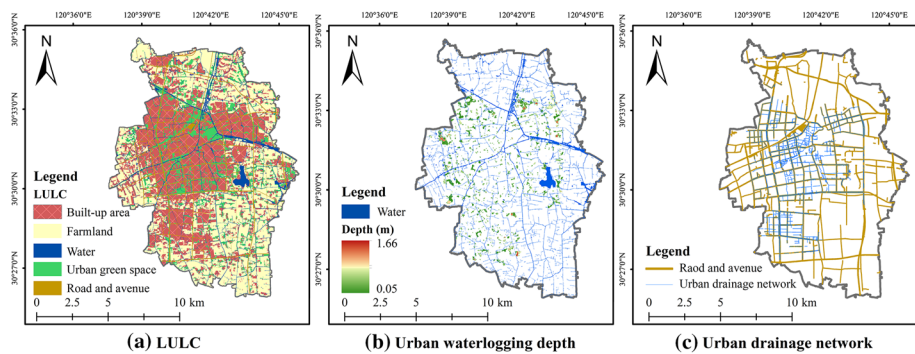


Fig. 5 The **a** land use and land cover, **b** urban waterlogging depth, and **c** urban drainage network

Table 4 Urban waterlogging statistics of different land cover

Land cover	Area (km ²)	Mean depth (m)	Submersed area (km ²)	Percentage of submersed area (%)
Built-up area	55.27	0.24	3.52	6.37
Road and avenue	8.30	0.19	0.63	7.59
Urban green space	17.58	0.22	0.79	4.49
Farmland	59.34	0.27	1.49	2.51

3 Results

3.1 Urban waterlogging depth (UWD)

The land use and land cover (LULC) map (Fig. 5a) showed that the built-up area was highly concentrated in the central and southern parts of the study area, with lumps and strips of urban green space distributed in it, while a large area of farmland was distributed in the north, west and southeast of the urban area. The results of the simulation (Fig. 5b) showed that when the rainfall period was 50 years, the maximum UWD reached 1.66 m. A large area of urban waterlogging was mainly distributed in the edge of the city, including the northeast, west, south the built-up area. On the contrary, the distribution of urban waterlogging in central city was scattered and less severe than the case in the edge of the city.

The statistical urban waterlogging conditions of each land cover are listed in Table 4. Comparing the mean depth, the depth of urban waterlogging in farmland was the largest, followed by built-up area, urban green space and road and avenue. The submersed area of built-up area was the largest reaching 3.52 km², which was the largest among all the categories. It is worth noting that the submerged area of farmland which has a close relationship with crops reached 1.49 km², ranking second. It is obvious that the submerged percentage of built-up areas and roads was significantly higher than that of urban green space and farmland, revealing the difference of the influence of pervious surface and impervious surface on urban waterlogging.

3.2 UWD and landscape composition

The Pearson correlation coefficients are shown in Fig. 6. It revealed the relationship across four analysis scales between UWD and the explanatory variables selected in this study. Lines in different color represent different analysis scales. And the value of the coordinate axis represents the correlation coefficient of the corresponding factor. The stepwise regression model results of four analysis scales are shown in Table 5. It was used to detect the comprehensive effects of the factors selected in this study on urban waterlogging. And the adjusted R^2 of model at 400 m, 600 m and 800 m analysis scale were 0.723, 0.323 and 0.193, respectively.

As shown in Fig. 6, the correlation coefficients between UWD and PLNAD of each land cover varied from analysis scales. For built-up area, the significant correlation coefficients between UWD and PLAND were 0.105, 0.204, and 0.274 at 400 m, 600 m and 800 m analysis scale, respectively. For road and avenue, there were no significant correlation coefficients between UWD and PLAND. For urban green space, the significant correlation coefficients between UWD and PLAND were -0.105 , -0.161 , and -0.155 at 400 m, 600 m and 800 m analysis scale, respectively. For farmland, the correlation coefficient between UWD and PLAND was significant at 200 m and 800 m analysis scale, valuing 0.127 and 0.155, respectively. And for water, the correlation coefficients between UWD and PLAND was significant at 600 m analysis scale with a value of -0.156 , while in three stepwise regression models, there was no effective variable represents landscape composition.

3.3 UWD and landscape configuration

The relationship between UWD and landscape configuration is also shown in Fig. 6 and Table 5. For built-up area (Fig. 6a), except PD, the other five indices were correlated significantly with urban waterlogging depth. And the correlation was the strongest at 800 m analysis scale. The coefficient of LPI, TE, AREA_MN, SHAPE_MN, and COHESION was 0.267, -0.215 , -0.243 , -0.258 , and -0.257 , respectively. In stepwise regression model (Table 5), the SHAPE_MN of built-up area was an effective variable at 800 m analysis scale. The standard regression coefficient was -0.216 . For road and avenue (Fig. 6b), the LPI, AREA_MN, SHAPE_MN, and COHESION were correlated significantly with urban waterlogging depth. And the correlation was the strongest at 800 m analysis scale. The coefficient of these indices was -0.186 , -0.209 , -0.166 , and -0.241 , respectively. The regression model showed that the PD of road and avenue was an effective variable at 400 m and 600 m analysis scale. The standard regression coefficient was 0.778 and 0.192, respectively.

For urban green space (Fig. 6c), except PD, the other five indices were correlated significantly with urban waterlogging depth. The correlation between TE and UWD was strongest at 600 m analysis scale with the coefficient of -0.164 , while LPI, AREA_MN, SHAPE_MN, and COHESION had the strongest correlation with UWD at 800 m analysis scale. The coefficient was -0.168 , -0.172 , -0.207 , and -0.156 , respectively. In regression model at 600 m and 800 m analysis scale, the standard coefficient of TE and LPI was -0.377 and -0.256 , respectively. For farmland (Fig. 6d), except TE and CHOESION, the other four indices were correlated significantly with urban waterlogging depth. The correlation between PD and UWD was strongest at 400 m analysis scale. And the coefficient was -0.227 , while LPI, AREA_MN, and SHAPE_MN had the strongest correlation with UWD at 800 m analysis scale. The

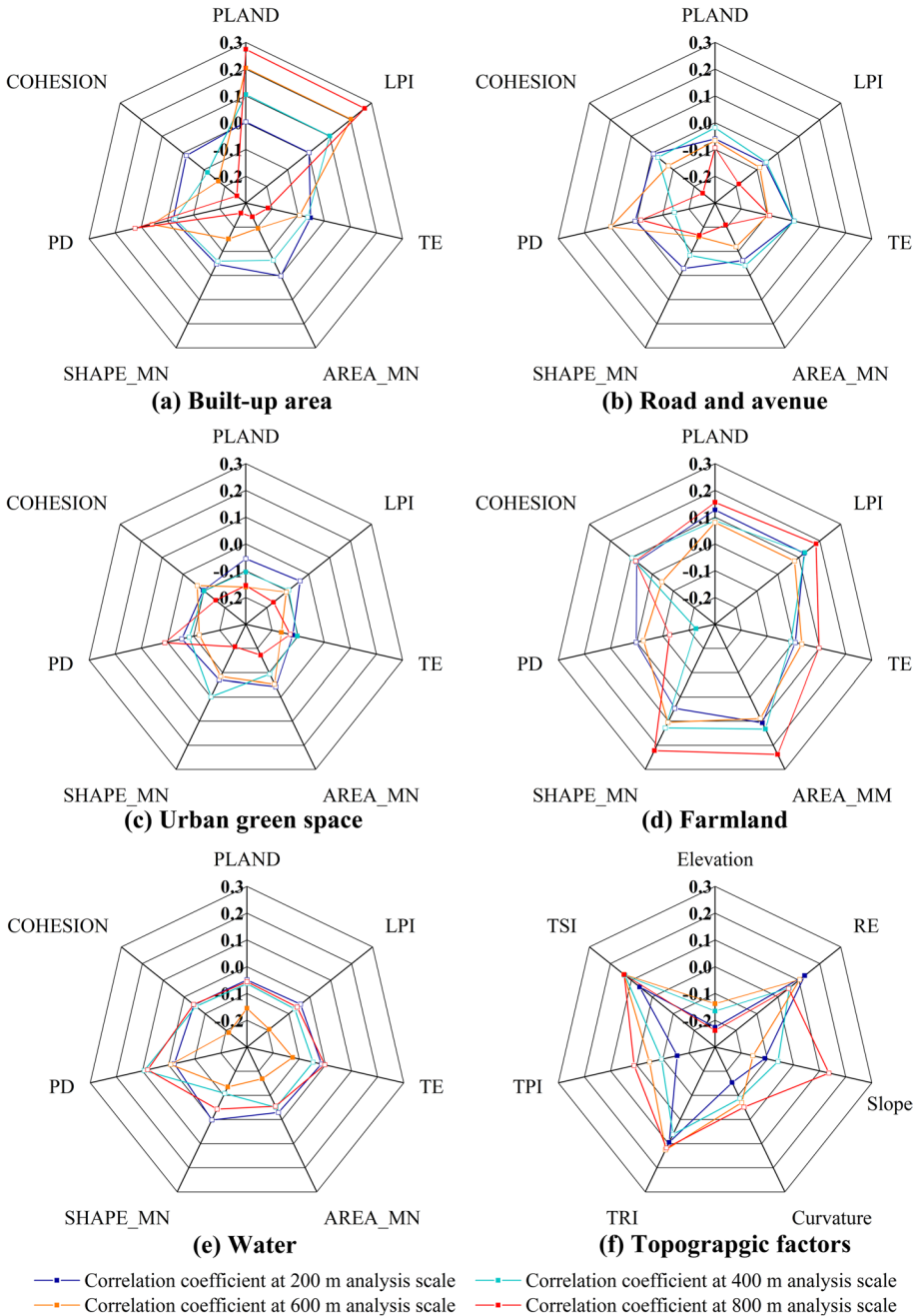


Fig. 6 The correlation coefficients between urban waterlogging depth and landscape composition and configuration, topographic factors across four analysis scales

Table 5 Stepwise regression model across four analysis models

400 m						
Variable	Elevation	AREA_ MN _{Farmaland}	PD _{RAV}	SHAPE_MN _{Farmland}	Inter- cept: -5.543	Adjusted R ² : 0.732
Regression coefficient	-2.138	0.608	0.778	-0.985		
VIF	1.726	2.567	1.441	3.542		
600 m						
Variable	RE	Elevation	PD _{RAV}	COHESION _{Water}	TE _{UGS}	Inter- cept: -2.007
regression coefficient	0.248	-0.324	0.192	-0.374	-0.377	Adjusted R ² : 0.323
VIF	2.594	3.861	1.367	5.953	4.571	
800 m						
Variable	Slope	AREA_MN _{UGS}	LPI _{UGS}	SHAPE_ MN _{Built-up area}	Intercept: -2.605	Adjusted R ² : 0.193
regression coefficient	0.144	-0.613	-0.256	-0.216		
VIF	1.958	2.579	4.358	2.647		

regression model showed that AREA_MN and SHAPE_MN of farmland were effective variables at 400 m analysis scale.

The landscape indices of water were special. There only existed significant correlation with UWD at 600 m analysis scale. The coefficient of LPI, TE, AREA_MN, SHAPE_MN, and COHESION were -0.194, -0.125, -0.169, -0.135, and -0.213, respectively. The regression model also showed the influence of COHESION of water on urban waterlogging at 600 m analysis scale.

3.4 UWD and topographic factors

From Fig. 6f, we can see that the elevation and TSI were significantly correlated with the UWD across four analysis scale. The correlation coefficients between UWD and elevation were -0.226, -0.166, -0.138, and -0.238, respectively, and TSI was 0.062, 0.130, 0.135, and 0.134, respectively, while RE (0.128), slope (-0.109), curvature (-0.153), TRI (0.095), and TPI (-0.155) were only significantly correlated with UWD at 200 m analysis scale.

4 Discussion

4.1 Correlations between urban waterlogging and landscape composition

Previous studies have shown that land covers and its ratios have an impact on urban waterlogging due to their surface heterogeneity (Zhang et al. 2021c). The research in southeast of China showed a positive correlation between waterlogging point density and percentage of built-up area, while the correlation between waterlogging point density and percentage of urban green space was negative (Wu and Zhang 2017; Zhang et al. 2018a). Consistent with the literature mentioned above, our research found that

the correlations between UWD and percentage of built-up area and urban green space were positive and negative at different analysis scales. As a representative of impervious surface, the built-up area accelerates the accumulation of surface runoff and cuts off the infiltration of surface water, which increases the risk of urban waterlogging, while the urban green space plays a completely opposite role. Besides, the result of our study showed a negative relationship between UWD and the percentage of water body, indicating that water body played a significant role on the reducing of urban waterlogging. It has also been reported in other case studies (McMinn et al. 2010; Zheng et al. 2016). Therefore, increasing the percentage of urban green space and water body in the process of urbanization can effectively reduce the risk of waterlogging.

As for road and avenue, the correlation analysis results did not show a significant correlation. It is supposed that the main reason was the area ratio of road and avenue was much smaller than other land covers in each analytical scale. Strangely, from the result of UWD results of each land cover, we found that as a kind of impervious surface, the mean UWD of the road and avenue was smaller than that of the urban green space (Table 4). The high density of municipal drainage facilities on the road and avenue may be the main reason for the minimum UWD (Fig. 5c). In order to test our hypothesis, two sample plots with similar landscape pattern and terrain were selected to compare the effect of urban drainage network on road accumulation water. The result show that, in sample plot 1 with high drainage network density, the road did not be submersed and there was no waterlogging area (Fig. 7a), while in sample plot 2, there were large areas of road were submersed and the largest depth was 0.07 m (Fig. 7b). Despite the positive role of the drainage system, the percentage of submersed area of road and avenue was the highest (Table 4). Therefore, we need to pay attention to the waterlogging risk on road and avenue, especially those in low drainage network density area.

The mean UWD of farmland was 0.27 m and ranked first at four land cover types (Table 4). There were two reasons to explain this phenomenon: (1) most of the farmland in the study area was paddy field, which can be seen as a man-made water storage area; (2) most of the farmland areas were in the suburbs, and the drainage network were lacking or backward. The result of Person correlation analysis also showed the positive relationship between UWD and the percentage of farmland. And this result was in agreement with pervious findings which showed the positive correlation between flood frequency and increasing of farmland (Du et al. 2015). Thus, controlling the percentage of farmland was a direct action to reduce the risk of waterlogging. However, the regulation of arable land minimum in China forced us to change our perspective of solving the problem to other aspects, such as optimizing farmland drainage systems and farmland spatial configuration (Ren et al. 2021).

4.2 Correlations between urban waterlogging and landscape configuration

The landscape configuration was significantly related to the UWD (Fig. 8), indicating that the spatial form of landscape patches strongly affects water accumulation on land surface. LPI indices measured the dominance of the single largest land cover patch (McGarigal and Marks 1995). Our study clearly showed that the LPI of built-up area and farmland correlated with UWD positively, while the LPI of road and avenue, urban green space, and water bodies were negatively correlated with UWD (Fig. 8a). These results were similarity to the findings in Pearl River Delta (Liu et al. 2021). As for impervious surface, larger single built-up patches have a stronger effect on reducing

(a) Sample plot 1

(b) Sample plot 2

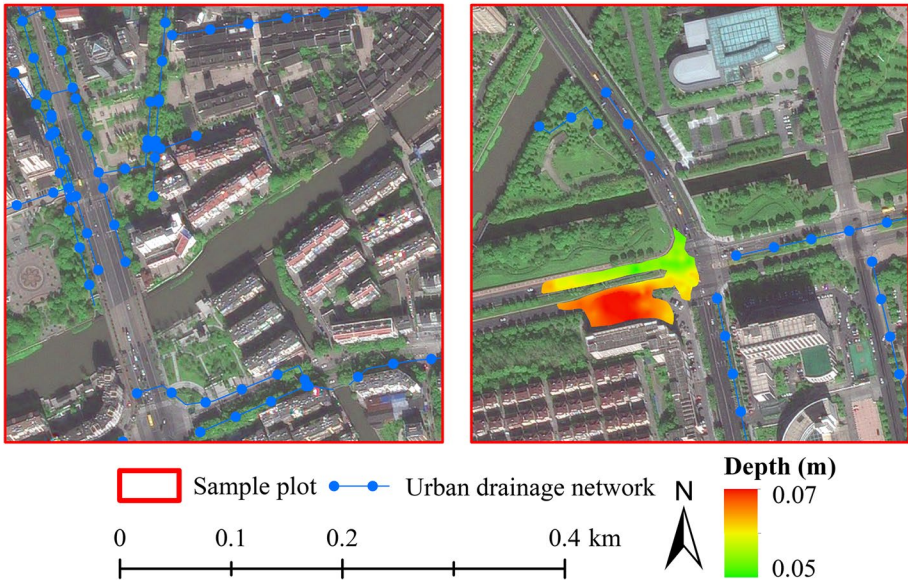


Fig. 7 The mitigation effect of urban drainage network on road accumulation water

rainwater infiltration, resulting in more surface runoff. At the same time, the higher runoff coefficient in built-up areas makes the UWD much deeper than other patches (Gao et al. 2020). Most of the farmland types in study area are paddy fields. It can be seen as artificial water storage area. Therefore, it was reasonable that the LPI of farmland was positively correlated with the UWD during rainfall process. Although considered as an impervious surface, the LPI of road and avenue was negatively correlated with urban waterlogging depth, in contrary to built-up area. Generally speaking, since the road patch shape was usually a banded, the larger the LPI is, the wider of the roads are. Wider roads and avenues were often of great significance or newly built in the city and generally have better drainage network. As a result, the correlation between UWD and the LPI of built-up area and roads showed an opposite trend. As for urban green space, a larger single patch will strengthen the effect of interception and infiltration of rainfall (Liu et al. 2020). Therefore, with the increase in LPI of urban green space, the UWD decreased. And for water bodies, a larger single patch could store more rainfall, thus reducing the other land covers' pressure of waterlogging.

TE indices measured the sum edge length of each land cover's patch. A larger TE indicates that the patch has longer boundaries with other patches, and the exchange of matter and energy is more frequently. And the SHAPE_MN indices measured the geometric complexity of the landscape (McGarigal and Marks 1995). The results of our study showed that UWD correlated negatively with TE and SHAPE_MN of built-up area, urban green space and water bodies (Fig. 8b, d). This suggested that massive patches which have longer edges and more complex shapes could reduce the UWD. One possible reason was that in the case of the same patch area, the patch with longer edge length and complex spatial shapes made the runoff disperse gradually as it flows across the boundary. In this context, the surface water had sufficient time to infiltrate causing the final reduce in surface water.

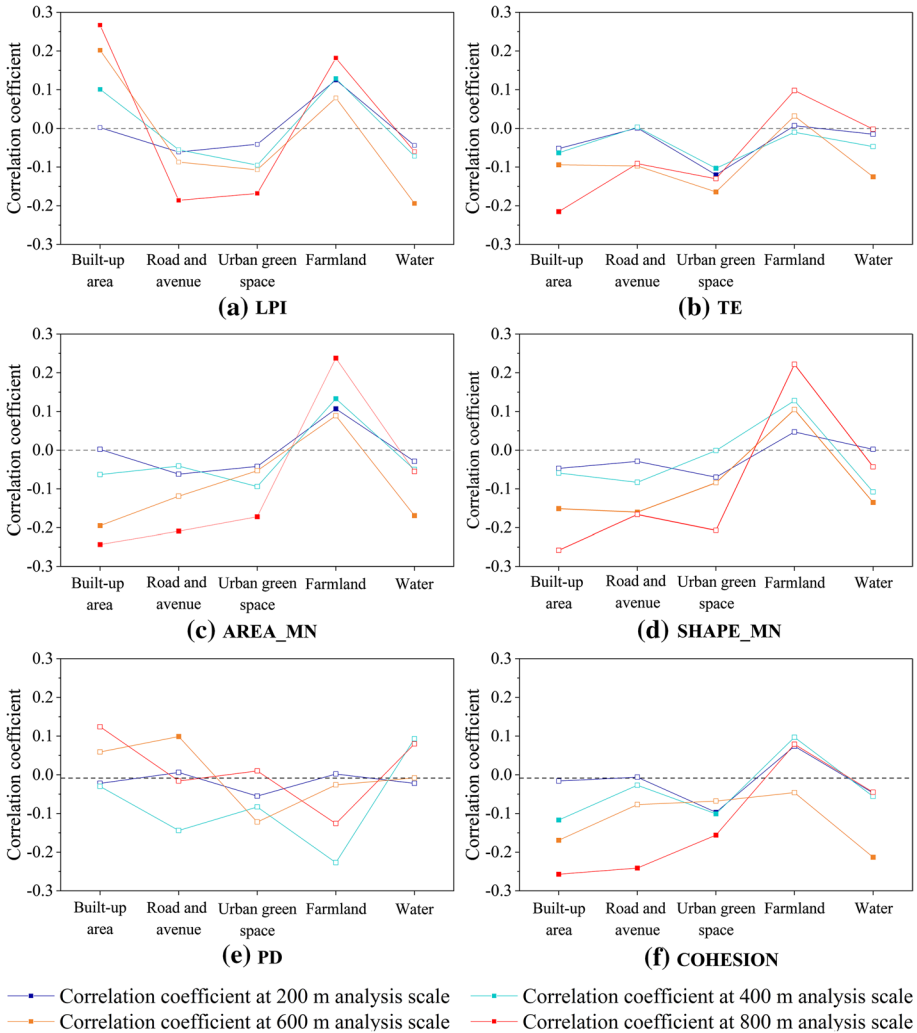


Fig. 8 The landscape indices and urban waterlogging depth

AREA_MN indices measured the average condition of patch size and was directly related to the number of patches of each land cover type. AREA_MN usually express the degree of fragmentation and the connectivity of landscape together with PD and CHOESION (McGarigal and Marks 1995). According to the results of our study, farmland patches with higher fragmentation and lower connectivity level could better reduce the urban waterlogging depth. Previous studies have reported that a certain type of land cover with fragmented patches may increase the exchange of soil and groundwater flows among the patches, thus decreasing the runoff (Liu et al. 2020). Contrarily, lower fragmentation and high connectivity level urban green space and water bodies were effective landscapes due to their stronger infiltration and water storage. Unexpectedly, the UWD was also correlated positively with fragmentation and negatively with connectivity of built-up areas and roads and avenue (Fig. 8c, e, f). We suspected that it was affected by the drainage network.

According to the stepwise regression models, the influence of landscape configuration on the UWD was stronger than that of landscape composition, especially the indices which characterize the shape and fragmentation of a landscape. Thus, in the perspective of planning landscape to reduce the risk of waterlogging, more attention should be paid to landscape configuration.

4.3 Correlations between urban waterlogging and topographic factors

The topographic factors have been widely used in assessment of urban waterlogging risk which proved the strong correlation between them (Yin et al. 2011; Quan 2014). Our study revealed their relationship quantitatively (Table 6). Through the analysis of the significant correlation coefficient, we found that the region with low altitude and flat or low-lying terrain have deeper UWD. However, these places were ideal areas for urban planners to layout a large number of buildings, which might further aggravate the pressure of urban waterlogging risk during heavy storm or rainfall season. Thus, increasing the surface gradient change within the city reasonably can effectively reduce the UWD and the risk of waterlogging. For example, tilting the urban topography to natural drainage and water storage facilities (rivers and lakes) to take maximum advantage their positive ability in hydrology process. And it was also a reasonable measure to reduce the height of the road so that more runoff could flow into the drainage pipe. Besides, we should make full and dual use of landscape pattern and topography, configure more permeable landscapes in low-lying areas.

4.4 Scale effect on correlations between urban waterlogging and impact factors

Multi-scale landscape pattern analysis is widely used in ecosystem service value, urban heat island, water quality change, and other fields to better explain the relationship between landscape pattern and the environmental indicators (Bai et al. 2020; Song et al. 2020; Wu and Lu 2021). Our study also emphasized the scale effect between UWD and its impact factors. The regression model could explain 72.3% variation in the UWD at 400 m spatial scale, while at 600 m and 800 m, the explanatory power of the regression models dropped

Table 6 Correlation coefficients between water accumulation depth and topographic factors across four analysis scales

Topographic factors	Analysis scales			
	200 m	400 m	600 m	800 m
Elevation	-0.226**	-0.166*	-0.138*	-0.238**
RE	0.128**	0.055	0.104	0.051
Slope	-0.109**	-0.059	-0.155	0.136
Curvature	-0.153**	-0.087	-0.070	-0.051
TRI	0.095**	0.062	0.126	0.118
TPI	-0.155**	-0.095	-0.049	0.010
TSI	0.062*	0.130**	0.135*	0.134*

***Represents *p* value < 0.001. **represents *p* value < 0.01. *represents *p* value < 0.05

sharply, to only 32.3% and 19.3%, respectively (Table 5). Besides, comparing the standard regression coefficient of each model, we found that the importance of topographic factors in the model decreased significantly with the increasing of spatial scale. The correlation coefficients between UWD and topographic factors also showed a significant relationship at small scales (200 m and 400 m). These all proved that the topography had an important influence on the UWD at small scales. In terms of landscape composition, the scale effect only existed in the categories of built-up area and urban green space. However, the correlation coefficient between the UWD and the proportion of built-up area was more sensitive to the change of scale than the proportion of urban green space. The scale effect of landscape configuration was also found in our study, especially the spatial pattern of built-up area. With the increasing of spatial scale, the LPI, TE and COHESION of built-up area were correlated with UWD stronger. Therefore, in the process of alleviating urban waterlogging risk through landscape reorganization, decision makers should fully consider the scale effect of each land cover type especially the built-up area, in order to achieve the maximum effects.

4.5 Limitations and future perspectives

Several limitations should be addressed to better understanding the results. First, the impact factors of UWD may be different under the different rainfall conditions. Our study only focused on the situation where the return period of rainfall was 50 years. More attention on rainfall conditions and climate change should be paid in the future work. Second, although the statistical analysis using the regular grid as the analysis unit could obtain the relationship between the UWD and the explanatory variables, the suggestions based on this may bring inconvenience because of the different management units in the actual rectification and reform work. Therefore, taking the management unit as the basic analysis unit will be better for the application of results. Finally, our research may not be able to reflect the urban waterlogging caused by the overloading of the sewage system caused by rainfall due to the lack of sewage network data.

5 Conclusion

Revealing the impact factors of urban waterlogging is of great significance to optimize the urban waterlogging prevention and management. In this study, the UWD simulated by InfoWorks ICM was used as a dependent variable to characterize urban waterlogging. And we conducted a method that combines the Pearson correlation analysis and stepwise regression model to investigate the relative contributions of impact factors to urban waterlogging through multi-scale study. There are four conclusions gained in study: (1) In terms of landscape composition, the influence of proportion of built-up area on urban waterlogging is the most significant among the five types of land covers, and the second is proportion of urban green space. This suggested that adjusting the proportion of built-up area and urban green space is an effective measure to reduce the risk of waterlogging. Meanwhile, the UWD results on the road show that the urban drainage network can effectively alleviate the local waterlogging. (2) The influence of landscape configuration variables on waterlogging is the most important among the landscape composition, configuration and topography. This result indicates that the urban waterlogging can be mitigated by optimizing the

spatial configuration of landscape. Average built-up area patch sizes and construct a larger single green space with complex shape and high connectivity can reduce the urban waterlogging risk. (3) At small scale, more attention should be paid to the role of topography factors, and the risk of urban waterlogging should be mitigated through the rational allocation of terrain gradient. (4) Across different scales of analysis, the correlation coefficient, regression model and its adjusted determination coefficients (Adjusted R^2) showed a strong scale effect. In this context, it is necessary to carry out multi-scale analysis, determine the main factors, and put forward reasonable solutions under the corresponding scales.

Acknowledgements The authors are very grateful for funding provided by Zhejiang Provincial Natural Science Foundation of China (LY19D010004), National Nature Sciences Foundation of Hangzhou (20191203B19).

Funding The authors have not disclosed any funding.

Declarations

Conflict of interest The authors declare that they have no known competing financial interests or personal relationships that could have appeared to influence the work reported in this paper.

References


- Abbas A, Salloom G, Ruddock F et al (2019) Modelling data of an urban drainage design using a Geographic Information System (GIS) database. *J Hydrol* 574:450–466. <https://doi.org/10.1016/j.jhydrol.2019.04.009>
- Babaei S, Ghazavi R, Erfanian M (2018) Urban flood simulation and prioritization of critical urban sub-catchments using SWMM model and PROMETHEE II approach. *Phys Chem Earth* 105:3–11. <https://doi.org/10.1016/j.pce.2018.02.002>
- Bai Y, Chen Y, Alatalo JM et al (2020) Scale effects on the relationships between land characteristics and ecosystem services- a case study in Taihu Lake Basin. *China Sci Total Environ* 716:137083. <https://doi.org/10.1016/j.scitotenv.2020.137083>
- Bisht DS, Chatterjee C, Kalakoti S et al (2016) Modeling urban floods and drainage using SWMM and MIKE URBAN: a case study. *Nat Hazards* 84:749–776. <https://doi.org/10.1007/s11069-016-2455-1>
- Burger G, Sitzenfrey R, Kleidorfer M, Rauch W (2014) Parallel flow routing in SWMM 5. *Environ Model Softw* 53:27–34. <https://doi.org/10.1016/j.envsoft.2013.11.002>
- Chen Y, Zhou H, Zhang H et al (2015) Urban flood risk warning under rapid urbanization. *Environ Res* 139:3–10. <https://doi.org/10.1016/j.envres.2015.02.028>
- Cheng T, Xu Z, Hong S, Song S (2017) Flood risk zoning by using 2D hydrodynamic modeling: a case study in Jinan City. *Math Probl Eng*. <https://doi.org/10.1155/2017/5659197>
- De Reu J, Bourgeois J, Bats M et al (2013) Application of the topographic position index to heterogeneous landscapes. *Geomorphology* 186:39–49. <https://doi.org/10.1016/j.geomorph.2012.12.015>
- Du S, Van Rompaey A, Shi P, Wang J (2015) A dual effect of urban expansion on flood risk in the Pearl River Delta (China) revealed by land-use scenarios and direct runoff simulation. *Nat Hazards* 77:111–128. <https://doi.org/10.1007/s11069-014-1583-8>
- Du S, Xiong Z, Wang Y, Guo L (2016) Remote sensing of environment quantifying the multilevel effects of landscape composition and configuration on land surface temperature. *Remote Sens Environ* 178:84–92. <https://doi.org/10.1016/j.rse.2016.02.063>
- Fahy B, Brenneman E, Chang H, Shandas V (2019) Spatial analysis of urban flooding and extreme heat hazard potential in Portland. *Or Int J Disaster Risk Reduct* 39:101117. <https://doi.org/10.1016/j.ijdrr.2019.101117>
- Gao F, He B, Xue S, Li Y (2020) Impact of landscape pattern change on runoff processes in catchment area of the Ulungur River Basin. *Water Sci Technol Water Supply* 20:1046–1058. <https://doi.org/10.2166/ws.2020.027>

- Hou H, Wang R, Murayama Y (2019) Scenario-based modelling for urban sustainability focusing on changes in cropland under rapid urbanization: a case study of Hangzhou from 1990 to 2035. *Sci Total Environ* 661:422–431. <https://doi.org/10.1016/j.scitotenv.2019.01.208>
- Hu T, Fan J, Hou H et al (2021) Long-term monitoring and evaluation of land development in a reclamation area under rapid urbanization: a case-study in Qiantang New District, China. *L Degrad Dev* 32:3259–3271. <https://doi.org/10.1002/ldr.3980>
- Huang T, Wang Y, Zhang J (2017) Simulation and evaluation of low impact development of urban residential district based on SWMM and GIS. *IOP Conf Ser Earth Environ Sci*. <https://doi.org/10.1088/1755-1315/74/1/012009>
- Huong HTL, Pathirana A (2013) Urbanization and climate change impacts on future urban flooding in Can Tho city. *Vietnam Hydrol Earth Syst Sci* 17:379–394. <https://doi.org/10.5194/hess-17-379-2013>
- H. Wallingford (2012), InfoWorks ICM help v3.0. UK
- Iwahashi J, Pike RJ (2007) Automated classifications of topography from DEMs by an unsupervised nested-means algorithm and a three-part geometric signature. *Geomorphology* 86:409–440. <https://doi.org/10.1016/j.geomorph.2006.09.012>
- Kirtman B, Power SB, Adedoyin AJ, et al (2013) Near-term climate change: projections and predictability. *Clim Chang* 2013 Phys Sci Basis Work Gr I Contrib to Fifth Assess Rep Intergov Panel Clim Chang 9781107057:953–1028. <https://doi.org/10.1017/CBO9781107415324.023>
- Li Y, Hu T, Zheng G et al (2019) An improved simplified urban storm inundation model based on urban terrain and catchment modification. *Water (switzerland)* 11:1–16. <https://doi.org/10.3390/w11112335>
- Liu F, Liu X, Xu T et al (2021) Driving factors and risk assessment of rainstorm waterlogging in urban agglomeration areas: a case study of the guangdong-hong kong-macao greater Bay area. *China Water (switzerland)*. <https://doi.org/10.3390/w13060770>
- Liu J, Liu X, Wang Y et al (2020) Landscape composition or configuration: which contributes more to catchment hydrological flows and variations? *Landsc Ecol* 35:1531–1551. <https://doi.org/10.1007/s10980-020-01035-3>
- Liu S, Lin M, Li C (2019) Analysis of the effects of the river network structure and urbanization on waterlogging in high-density urban areas—a case study of the Pudong New Area in Shanghai. *Int J Environ Res Public Health*. <https://doi.org/10.3390/ijerph16183306>
- McGarigal K, Marks BJ (1995) FRAGSTATS: spatial pattern analysis program for quantifying landscape structure. *Gen Tech Rep US Dep Agric for Serv*. <https://doi.org/10.2737/PNW-GTR-351>
- McMinn WR, Yang Q, Scholz M (2010) Classification and assessment of water bodies as adaptive structural measures for flood risk management planning. *J Environ Manag* 91:1855–1863. <https://doi.org/10.1016/j.jenvman.2010.04.009>
- Nayeb Yazdi M, Ketabchy M, Sample DJ et al (2019) An evaluation of HSPF and SWMM for simulating streamflow regimes in an urban watershed. *Environ Model Softw* 118:211–225. <https://doi.org/10.1016/j.envsoft.2019.05.008>
- Quan RS (2014) Rainstorm waterlogging risk assessment in central urban area of Shanghai based on multiple scenario simulation. *Nat Hazards* 73:1569–1585. <https://doi.org/10.1007/s11069-014-1156-x>
- Ren X, Wang S, Yang P et al (2021) Performance evaluation of different combined drainage forms on flooding and waterlogging removal. *Water (switzerland)* 13:1–15. <https://doi.org/10.3390/w13212968>
- Sang YF, Yang M (2017) Urban waterlogs control in China: more effective strategies and actions are needed. *Nat Hazards* 85:1291–1294. <https://doi.org/10.1007/s11069-016-2614-4>
- Shi Y, Zhai G, Zhou S et al (2019) How can cities respond to flood disaster risks under multi-scenario simulation? A case study of Xiamen, China. *Int J Environ Res Public Health*. <https://doi.org/10.3390/ijerph16040618>
- Sidek LM, Jaafar AS, Majid WHAWA et al (2021) High-resolution hydrological-hydraulic modeling of urban floods using infoworks icm. *Sustain*. <https://doi.org/10.3390/su131810259>
- Song J, Wang J, Xi G, Lin H (2021) Evaluation of stormwater runoff quantity integral management via sponge city construction: a pilot case study of Jinan. *Urban Water J* 18:151–162. <https://doi.org/10.1080/1573062X.2020.1860237>
- Song Y, Song X, Shao G (2020) Effects of green space patterns on urban thermal environment at multiple spatial-temp. *Sustain*. <https://doi.org/10.3390/SU12176850>
- Su B, Huang H, Li Y (2016) Integrated simulation method for waterlogging and traffic congestion under urban rainstorms. *Nat Hazards* 81:23–40. <https://doi.org/10.1007/s11069-015-2064-4>
- Tang X, Shu Y, Lian Y et al (2018) A spatial assessment of urban waterlogging risk based on a Weighted Naïve Bayes classifier. *Sci Total Environ* 630:264–274. <https://doi.org/10.1016/j.scitotenv.2018.02.172>
- Tehrany MS, Jones S, Shabani F (2019) Identifying the essential flood conditioning factors for flood prone area mapping using machine learning techniques. *CATENA* 175:174–192. <https://doi.org/10.1016/j.catena.2018.12.011>

- Wang H, Zhao Y, Zhou Y, Wang H (2021) Prediction of urban water accumulation points and water accumulation process based on machine learning. *Earth Sci Inf* 14:2317–2328. <https://doi.org/10.1007/s12145-021-00700-8>
- Wang L, Hou H, Weng J (2020) Ordinary least squares modelling of urban heat island intensity based on landscape composition and configuration: a comparative study among three megacities along the Yangtze River. *Sustain Cities Soc* 62:102381. <https://doi.org/10.1016/j.scs.2020.102381>
- Wang Z, Lai C, Chen X et al (2015) Flood hazard risk assessment model based on random forest. *J Hydrol* 527:1130–1141. <https://doi.org/10.1016/j.jhydrol.2015.06.008>
- Wu J, Lu J (2021) Spatial scale effects of landscape metrics on stream water quality and their seasonal changes. *Water Res* 191:116811. <https://doi.org/10.1016/j.watres.2021.116811>
- Wu J, Sha W, Zhang P, Wang Z (2020) The spatial non-stationary effect of urban landscape pattern on urban waterlogging: a case study of Shenzhen City. *Sci Rep* 10:1–15. <https://doi.org/10.1038/s41598-020-64113-1>
- Wu J, Zhang P (2017) The effect of urban landscape pattern on urban waterlogging. *Dili Xuebao/Acta Geogr Sin* 72:444–456. <https://doi.org/10.11821/dlxb201703007>
- Xue F, Huang M, Wang W, Zou L (2016) Numerical simulation of urban waterlogging based on FloodArea model. *Adv Meteorol*. <https://doi.org/10.1155/2016/3940707>
- Yang Y, Ng ST, Dao J et al (2021) BIM-GIS-DCEs enabled vulnerability assessment of interdependent infrastructures—a case of stormwater drainage-building-road transport Nexus in urban flooding. *Autom Constr* 125:103626. <https://doi.org/10.1016/j.autcon.2021.103626>
- Yao L, Chen L, Wei W (2017) Exploring the linkage between urban flood risk and spatial patterns in small urbanized catchments of Beijing, China. *Int J Environ Res Public Health*. <https://doi.org/10.3390/ijerph14030239>
- YE C, XU Z, LEI X, et al (2021) Flood simulation and risk analysis based on infoworks ICM: case study in the Baima River District of Fuzhou City. *J Beijing Norm Univ Sci* 57:5–8+73. <https://doi.org/10.12202/j.0476-0301.2021088>
- Yin Z, Yin J, Xu S, Wen J (2011) Community-based scenario modelling and disaster risk assessment of urban rainstorm waterlogging. *J Geogr Sci* 21:274–284. <https://doi.org/10.1007/s11442-011-0844-7>
- Yu H, Zhao Y, Fu Y, Li L (2018) Spatiotemporal variance assessment of urban rainstorm waterlogging affected by impervious surface expansion: a case study of Guangzhou. *China Sustain*. <https://doi.org/10.3390/su10103761>
- Zambrano L, Pacheco-Muñoz R, Fernández T (2018) Influence of solid waste and topography on urban floods: the case of Mexico City. *Ambio* 47:771–780. <https://doi.org/10.1007/s13280-018-1023-1>
- Zhang H, Cheng J, Wu Z et al (2018a) Effects of impervious surface on the spatial distribution of urban waterlogging risk spots at multiple scales in Guangzhou. *South China Sustain*. <https://doi.org/10.3390/su10051589>
- Zhang H, Wu C, Chen W, Huang G (2017) Assessing the impact of climate change on the waterlogging risk in coastal cities: a case study of Guangzhou, South China. *J Hydrometeorol* 18:1549–1562. <https://doi.org/10.1175/JHM-D-16-0157.1>
- Zhang H, Yang Z, Cai Y et al (2021a) Impacts of climate change on urban drainage systems by future short-duration design rainstorms. *Water (switzerland)*. <https://doi.org/10.3390/w13192718>
- Zhang Q, Wu Z, Guo G et al (2021b) Explicit the urban waterlogging spatial variation and its driving factors: the stepwise cluster analysis model and hierarchical partitioning analysis approach. *Sci Total Environ* 763:143041. <https://doi.org/10.1016/j.scitotenv.2020.143041>
- Zhang Q, Wu Z, Tarolli P (2021c) Investigating the role of green infrastructure on urban waterlogging: evidence from metropolitan coastal cities. *Remote Sens*. <https://doi.org/10.3390/rs13122341>
- Zhang Q, Wu Z, Zhang H et al (2020) Identifying dominant factors of waterlogging events in metropolitan coastal cities: the case study of Guangzhou. *China J Environ Manag* 271:110951. <https://doi.org/10.1016/j.jenvman.2020.110951>
- Zhang Y, Xia J, Yu J et al (2018b) Simulation and assessment of urbanization impacts on runoff metrics: insights from landuse changes. *J Hydrol* 560:247–258. <https://doi.org/10.1016/j.jhydrol.2018.03.031>
- Zhao G, Pang B, Xu Z et al (2018) Mapping flood susceptibility in mountainous areas on a national scale in China. *Sci Total Environ* 615:1133–1142. <https://doi.org/10.1016/j.scitotenv.2017.10.037>
- Zhao Y, Xia J, Xu Z et al (2021) Impact of urban expansion on rain island effect in jinan city, north china. *Remote Sens* 13:1–16. <https://doi.org/10.3390/rs13152989>
- Zheng Y, Li Y, Hou H et al (2021) Quantifying the cooling effect and scale of large inner-city lakes based on landscape patterns: a case study of hangzhou and nanjing. *Remote Sens*. <https://doi.org/10.3390/rs13081526>
- Zheng Z, Gao J, Ma Z et al (2016) Urban flooding in China: main causes and policy recommendations. *Hydrol Process* 30:1149–1152. <https://doi.org/10.1002/hyp.10717>

Publisher's Note Springer Nature remains neutral with regard to jurisdictional claims in published maps and institutional affiliations.

Authors and Affiliations

Luoyang Wang^{1,2} · Yao Li⁴ · Hao Hou^{1,2,3} · Yan Chen^{1,2} · Jinjin Fan^{1,2} · Pin Wang^{1,2,3} · Tangao Hu^{2,3} 

¹ School of Information Science and Technology, Hangzhou Normal University, Yuhangtang Road No. 2318, Hangzhou 311121, China

² Institute of Remote Sensing and Earth Sciences, Hangzhou Normal University, Yuhangtang Road No. 2318, Hangzhou 311121, China

³ Zhejiang Provincial Key Laboratory of Urban Wetlands and Regional Change, Yuhangtang Road No. 2318, Hangzhou 311121, China

⁴ Faculty of Geo-Information Science and Earth Observation (ITC), University of Twente, 7500 AE Enschede, The Netherlands